https://doi.org/10.5194/egusphere-2025-3780
Preprint. Discussion started: 18 August 2025

Marine eukaryote community responses to the climate and oceanographic changes in Storfjordrenna (southern Svalbard) over the past ~14.0 kyr BP: Insights from sedimentary ancient DNA analysis

Hasitha Nethupul[1*], Magdalena Łącka[1], Marek Zajączkowski[1], Dhanushka Devendra[1], Ngoc-Loi Nguyen[1], Jan Pawłowski[1], Joanna Pawłowska[1]

[1] Department of Palaeoceanography, Institute of Oceanology, Polish Academy of Sciences, Sopot 81-712, Poland

* *Correspondence to:* Hasitha Nethupul (nethupul@iopan.pl)

https://doi.org/10.5194/egusphere-2025-3780
Preprint. Discussion started: 18 August 2025

Abstract

Sedimentary ancient DNA (sedaDNA) metabarcoding is an emerging method to reconstructing the response of marine organisms to past climate and oceanographic changes, including rare and non-fossilized taxa. Marine *seda*DNA records from the Arctic are scarce, especially those focusing on the impact of environmental shifts on the biodiversity and functional composition of marine eukaryotes communities. Here, we present a sedaDNA eukaryotic record from the sediment core retrieved in Storfjordrenna, southern Svalbard, spanning the termination of the Bølling-Allerød, the Younger Dryas, and the Holocene (13.3 - 1.3 kyr BP). We successfully recovered the eukaryotic communities and identified them by their ecological roles. Our study showed that the eukaryotic biodiversity in Storfjordrenna remained relatively stable, except during transitions between major climatic intervals. These shifts were marked by changes in richness and relative abundance, driven by factors such as perennial ice cover, surface water cooling, and subsurface Atlantic water influx. Cercozoans and MAST emerged as dominant heterotrophs, characterized by high ecological flexibility and broad tolerance. The primary productivity was primarily driven by ArW-associated phytoplankton, including diatoms (*Thalassiosira* and *Chaetoceros*), green algae (*Micromonas*), and autotrophic dinoflagellates (*Polarella glacialis*,) as well as mixoplanktonic silicoflagellate *Pseudopedinella elastica*. The ASV-based indicator analysis revealed that uncultured Cercozoan lineages and MAST taxa were primarily associated with AW proxies, whereas parasitic dinoflagellates (Dino-group I) and choanoflagellates were more closely aligned with ArW proxies. The analysis of indicator responses shows the complex interactions within eukaryotic communities, and reveals a strong association among functional ecological groups, which impacts ecosystem productivity and regulation. This complexity highlights the limitations of traditional single proxy approaches to accurately reconstructing paleoenvironmental conditions. Our study demonstrates the potential of high-resolution marine sedaDNA metabarcoding in elucidating responses to past climate changes and in improving our understanding of the intricate interactions within eukaryotic communities in marine ecosystems.

https://doi.org/10.5194/egusphere-2025-3780
Preprint. Discussion started: 18 August 2025

1. Introduction

The Arctic marine ecosystem is undergoing rapid and profound changes, primarily driven by climate warming (Ipcc, 2023; Polyakov et al., 2017; Polyakov et al., 2020). A prominent feature of these changes is the increasing influx of Atlantic Water (AW) into the region, a phenomenon known as Atlantification. This process is associated with warming, rise of sea surface temperatures (SST), reduced sea-ice cover, alterations of salinity patterns, and changes in nutrient dynamics (Årthun et al., 2012; Polyakov et al., 2017).

These transformations in the marine environment are altering the biodiversity of Arctic region and impacting the function and resilience of ecosystems (Benner et al., 2019; Hallegraeff, 2010; Ribeiro et al., 2024). The Storfjordrenna region in southern Svalbard is an ideal location to study these shifts, having experienced significant climate-driven changes over the last ~14,000 years, driven by meltwater discharge and the interaction between cold Arctic Water (ArW) and warmer AW inflows (Łącka et al., 2019; Łącka et al., 2015; Pawlowska et al., 2020; Telesiński et al., 2024). The region's biodiversity has been shaped by, and remains sensitive to, these fluctuating and dynamic environmental conditions (Bensi et al., 2025; Deb and Bailey, 2023; Górska et al., 2022; Hop et al., 2019). Understanding how it adapts to such changes is essential for reconstructing past ecological responses to climate change and for predicting future trends. While the impact of climate change on Arctic marine ecosystems is well documented (Deb and Bailey, 2023; Wassmann et al., 2010), relatively few studies have explored marine ecosystems using sedimentary ancient DNA (sedaDNA) to assess long-term biodiversity patterns (Grant et al., 2024; Pawlowska et al., 2020; Zimmermann et al., 2023). Recent developments in sedaDNA techniques have increased our ability to extract and analyze DNA from marine environments, providing valuable insights into eukaryotic communities and their responses to environmental changes over geological time scales (Harðardóttir et al., 2024; Grant et al., 2024; Zimmermann et al., 2021). Studies of marine eukaryotic sedaDNA have demonstrated that even low-resolution records can provide significant data on the shifts in marine communities over time, offering a window into past ecosystem dynamics (Grant et al., 2024). For instance, recent studies have demonstrated the potential of the sedaDNA approach in reconstructing the interactions between sea-ice cover, ocean temperatures and eukaryotic community composition (Armbrecht, 2020; Grant et al., 2024; Harðardóttir et al., 2024; Zimmermann et al., 2023; Zimmermann et al., 2021). However, there remains a notable lack of suitable-resolution marine sedaDNA records from the Arctic, especially those focusing on the impact of environmental shifts on the biodiversity and functional composition of marine communities.

https://doi.org/10.5194/egusphere-2025-3780
Preprint. Discussion started: 18 August 2025

This study addresses this gap by reconstructing the long-term history of marine eukaryotic communities using sedaDNA metabarcoding analysis from Storfjordrenna, southern Svalbard. The sedaDNA record is supported by previously published sedimentological, micropaleontological and geochemical records (Łącka et al., 2019; Łącka et al., 2020; Łącka et al., 2015; Telesiński et al., 2024). By focusing on eukaryotic communities associated with ArW and AW masses, we aim to assess their structure, ecological roles, and potential as indicators of past environmental conditions. Our approach seeks to identify how marine ecosystem have responded to significant climate-driven changes in this region and how these responses can improve our understanding of the future trajectory of Arctic marine biodiversity in the context of ongoing climate warming.

2. Study area

Storfjorden is an open fjord system located in the Svalbard Archipelago, between the islands of Spitsbergen, Barentsøya, and Edgeøya (**Fig. 1a**). The cross-shelf through Storfjordrenna is located south of Storfjorden's mouth. The hydrography of Storfjorden and Storfjordrenna is primarily governed by the interplay of two major water masses: AW and ArW. AW is typically characterized by relatively warm temperatures (>3 °C) and high salinity (>34.95), whereas ArW exhibits lower temperatures (<0.5 °C) and salinity ranging from 34.3 to 34.8 (Bensi et al., 2025; Skogseth et al., 2020; Sundfjord et al., 2017). AW is transported northwards by the Norwegian Atlantic Current, which bifurcates upon entering the Barents Sea into the West Spitsbergen Current and the North Cape Current (Blindheim and Osterhus, 2005). In contrast, ArW enters the region via the East Spitsbergen Current and the Bear Island Current, bringing cold, less saline waters into the Barents Sea (Hopkins, 1991). AW enters Storfjordrenna in a cyclonic manner, following the bathymetry, and the Polar Front separating AW and ArW water masses is located along the slope of Storfjordrenna(Bensi et al., 2025).

https://doi.org/10.5194/egusphere-2025-3780
Preprint. Discussion started: 18 August 2025

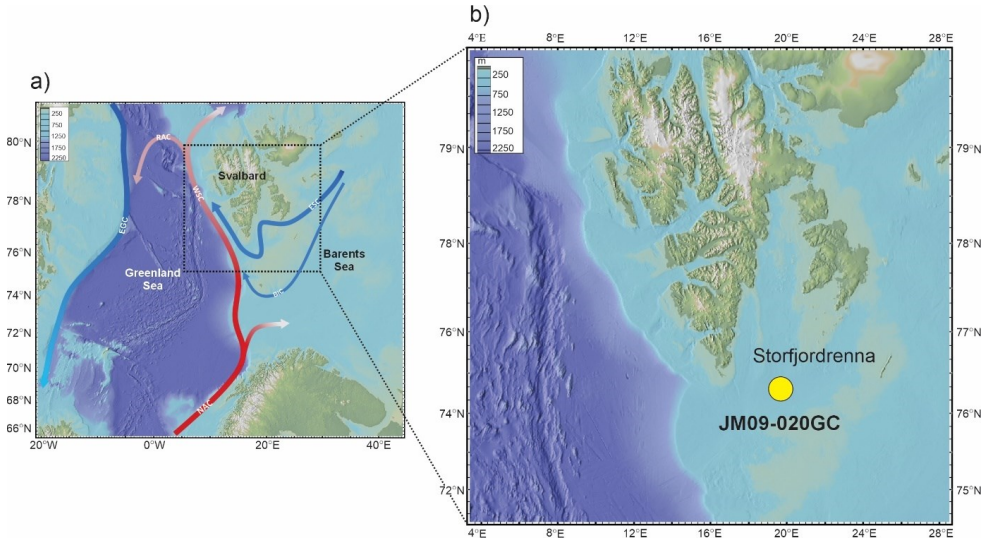

Figure 1. a) Map of the study area and (b) location of core JM09-020GC (yellow dot). Red arrows indicate warm currents, and blue arrows indicate cold currents. Abbreviations: NAC: North Atlantic Current, WSC: West Spitsbergen Current, RAC: Return Atlantic Current, ESC: East Spitsbergen Current, BIC: Bear Island Current, EGC: East Greenland Current.)

3. Materials and Methods

3.1 Sediment core and age model

Gravity core JM09-020-GC was collected in 2009 at a depth of 253 m in Storfjordrenna, northwestern Barents Sea during the expedition of R/V Jan Mayen (**Fig. 1b**). The core was stored and processed according to the methods described by (Łącka et al., 2019; Łącka et al., 2020; Łącka et al., 2015). The chronology of the core was established based on AMS ^{14}C radiocarbon dating. The dates published first by Łącka et al.(2015) were recalibrated using the Marine20 calibration curve (Heaton et al., 2020). The palaeoceanographic history of Storfjordrenna over the past ~14,000 years is well documented through detailed, multi-proxy reconstructions. These include analyses of fossil foraminifera assemblages, isotopic composition of foraminiferal tests, grainsize and elemental composition of sediments, alkenones (Łącka et al., 2019; Łącka et al., 2015), and dinoflagellate cysts (Telesiński et al., 2024).

3.2 SedaDNA workflow

3.2.1 DNA extraction, amplification, and sequencing

https://doi.org/10.5194/egusphere-2025-3780
Preprint. Discussion started: 18 August 2025

Approximately 10 g of sediment was collected from 55 sediment layers using sterile spoons and transferred to sterile containers. DNA extractions were performed using the DNeasy PowerMax Soil Kit (Qiagen), following the manufacturer's instructions. All DNA extracts were stored at −20°C until PCR amplification.

The V1V2 region of the 18S rDNA (with a length of ~340 bp) was amplified by PCR using the forward primer SSU_FO4mod (5′-GCT TGW CTC AAA GAT TAA GCC-3′) and the reverse primer SSU_R22 (3′-CCT GCT GCC TTC CTT RGA-5′) (Lindeque et al., 2013), which were tagged with a unique 8-nucleotide sequence at their 5′ ends. Each sample was amplified in triplicate and each PCR reaction was performed in a total volume of 25 µL, which included 1.5 µL of 1.5 mM MgCl2 (Applied Biosystems, USA), 2.5 µL of 10× PCR buffer II (Applied Biosystems), 0.5 µL of 0.2 mM deoxynucleotide triphosphates (Promega, USA), 0.5 µL of 20 mg/ mL bovine serum albumin (Invitrogen Ultrapure, USA), 1 µL of 10 µM of each primer, 0.2 µL of AmpliTaq Gold DNA polymerase (Applied Biosystems) and 2 µL of template DNA. The amplification conditions consisted of a pre-denaturation step at 95°C for 5 min, followed by 50 cycles of denaturation at 95°C for 30 s, annealing at 57°C for 30 s and extension at 72°C for 1 min, followed by a final extension step at 72°C for 5 min. PCR products, including negative control for each unique combination of tag-encoded primers, were verified by agarose gel electrophoresis. PCR products were purified using the High Pure PCR Cleanup Micro Kit (Roche) and quantified using a Qubit 2.0 fluorometer. Libraries were pooled in equimolar quantities and the sequence library was prepared using a TruSeq library-preparation kit (Illumina). Samples were then loaded into a MiSeq instrument for a paired-end run of 2*250 cycles. The sequencing was performed at the University of Geneva.

3.2.2 Data quality control and processing

The raw sequencing reads for each sample were processed using the SLIM web application (Dufresne et al., 2019). In brief, the module *demultiplexer* was used to demultiplex the raw reads according to their unique tag in the forward and reverse reads. Quality filtering, chimera removal and generation of the Amplicon Sequence Variants (ASVs) table were performed using DADA2 v.1.16 (Callahan et al., 2016) with pseudo-pool parameters.

The ASVs were curated using the LULU package v.0.1.0 (Froslev et al., 2017) with the default parameters. The taxa assignment of the ASVs was performed using VSEARCH against the taxonomically curated PR2 database v.4.14.1 (Guillou et al., 2013), which contains functional annotations. We used a Last Common Ancestor approach, assigning to the consensual taxonomic rank to up to reference sequences with at least 80% similarity. The ASVs

https://doi.org/10.5194/egusphere-2025-3780
Preprint. Discussion started: 18 August 2025

were also assigned to functional groups with at least 95% similarity; with the functional attributes of Ibarbalz et al., (2019). The ASVs assigned to prokaryotes (bacteria and archaea) were removed in order to analyze only eukaryotic ASVs. Additionally, fungi and gymnamoebae were removed due to the high risk of contamination (Armbrecht, 2020). Unique ASVs (occurring in only one sample), short sequences (<200 bp), rare ASVs (having <100 reads), and low read count samples (< 1000 reads) were removed from the dataset. Additionally, the unassigned sequences were blasted with NCBI to further clarify the taxonomic composition. The Cumulative Sum Scaling (CSS) technique was used to transform the read counts in the dataset and using 'cssNorm' function in the genomeSeq package (Paulson et al., 2013). CSSlog1p (scale factor - 0.75) was used for the downstream statistical analysis in the study.

3.3 Statistical analysis

Data analysis was performed in R v.4.2.2 (Team, 2013) using several R packages. The relative abundance of reads and ASVs of each eukaryote group were calculated and plotted using *ggplot2* (Wickham, 2016) and Grapher 24.1.213.

Three alpha diversity indices were calculated for all samples using the Hill number diversity (ASV richness q = 0, Shannon index q = 1, and Simpson index q = 2) based on the functions in the *hillR* packages (Chao et al., 2014). Hill-Shannon diversity was compared between the main groups using the Kruskal-Walli's rank test in the *stats* package (Kruskal and Wallis, 1952). The significance between the groups was determined using a pairwise Wilcoxon rank sum test with an adjusted p value (Benjamini-Hochberg) in the *ggpubr* package (Kassambara, 2023), and Permutational Multivariate Analysis of Variance (PERMANOVA) with 999 permutations via adonis2 function in the *vegan* package (Oksanen et al., 2007). A Principal Coordinate Analysis (PCoA) ordination was generated using the Bray-Curtis dissimilarity matrix calculated with the *ape* package (Paradis et al., 2019)and *stringer* package (Wickham, 2019) to assess beta diversity and visualize dissimilarities in eukaryotic community composition among the samples.

A co-occurrence heatmap representing most of families in the study was generated. The *corrplot* (Wei and Simko, 2024) and *pheatmap* packages were used based on spearman method the analyze the correlation between eukaryote families (a cutoff mark in correlation as > 0.5, and p value Benjamini-Hochberg (BH) adjusted < 0.05). Environmental parameters represented by paleoceanographic proxies were used to identify the response of eukaryote species through three analytical methods Seven proxies were used including indicators of sea surface temperature (SST U_{37}^{K*}) (Łącka et al., 2019), AW indicators foraminifera *Nonionellina*

https://doi.org/10.5194/egusphere-2025-3780
Preprint. Discussion started: 18 August 2025

labradorica and *Buccella frigida* (Łącka et al., 2015), dinocyst *Operculodinium centrocarpum* (Telesiński et al., 2024), ArW/meltwater indicator (%C37:4) (Łącka et al., 2019), glaciomarine condition indicator foraminifera *Elphidium excavatum* and *Cassidulina reniforme* (Łącka et al., 2015), sea ice indicators dinocysts *Echinidinium karaense* from (Telesiński et al., 2024), and bottom current dynamics (mean grain size 0-63 μm) (Łącka et al., 2015). Fuzzy set ordination (FSO) plots were generated for each environmental variable to assess their influence on eukaryote communities and identify key proxies for downstream analysis (Roberts, 2008). Firstly, a heatmap of sparse partial least squares (sPLS) regression between ASVs, and proxies was generated using the *spls* and *cim* function in *mixOmics* package (Froslev et al., 2017; Kim-Anh Lê Cao et al., 2008). The potential ASV based indicators were selected based on a correlation coefficient threshold of > 0.3 and BH adjusted p value of < 0.05. Secondly, a Spearman correlation heatmap of the top 100 most significant ASVs (rho > 0.3 and p-adjust < 0.05) as generated using the *pheatmap* package. Finally, the dataset was analyzed using DEseq2 analysis, and the dataset was curated based on log2FoldC ≥ 1 (BH-adjusted p value < 0.05), and lower base mean (Love et al., 2014). Potential indicator ASVs were categorized based on their correlation strength and consistent detection across at least two methods or strong association with multiple paleo-proxies.

4. Results

4.1 Metabarcoding data

A total of 2,620,808 raw sequence reads were generated from 55 samples. After filtering, 13 samples which mainly spanned the period between 4.0 and 7.5 kyr BP, were removed due to low number of reads. This reduced our dataset to 1,609,500 sequence reads and 273 ASVs in 42 samples (**Table S1, S2**).

4.2 Alpha diversity

Alpha diversity indices varied across time intervals, although Hill's Shannon diversity showed no significant differences (Kruskal-Wallis, $p = 0.48$; **Fig. S1, Table S1**). Overall, the number of observed ASVs ranged from 4 to 144 (**Fig. S1**). The highest values were observed in the Younger Dryas, Early Holocene and Late Holocene, particularly at 12.3 kyr BP, 11.3 kyr BP, 9.5 kyr BP, 4.0 kyr BP, and 2.8-2.3 kyr BP. In contrast, a significant decrease in richness was observed around 13.3 kyr BP, 11.8 kyr BP, 2.17 kyr BP, and 1.8 kyr BP (**Fig. S1 , Table S1**). Similar trends were revealed by both the Shannon and Simpson indices, with minimal diversity observed around 12.8 kyr, 11.7 kyr, 9.2 kyr, and 3.4 kyr BP. Between 11.7 kyr and

https://doi.org/10.5194/egusphere-2025-3780
Preprint. Discussion started: 18 August 2025

9.2 kyr BP. Due to limited data resolution, no clear trends in alpha diversity could be discerned between 9.2kyr and 3.4 kyr BP. However, a decline was evident after 3.4 kyr BP, continuing towards 1.3 kyr BP (**Fig. S1**).

4.3 Beta Diversity

Beta diversity analyses revealed minor changes in community composition during the transitions from the Bølling-Allerød to the Younger Dryas, and from the Younger Dryas to the Holocene (**Fig. 2**). The PCoA plot revealed overlap across different time intervals. Late Holocene and Younger Dryas samples were widely dispersed, while Early Holocene samples clustered separately along Axis 1, respectively. In contrast, Bølling-Allerød and Mid Holocene samples were largely scattered along the same axis (**Fig. 2**). PERMANOVA results supported significant differences in community composition ($p < 0.05$) between the Late and Early Holocene, Late Holocene and Younger Dryas, Early Holocene and Younger Dryas, and Younger Dryas and Bølling–Allerød (**Table S3**). FSO plots revealed a significant relationship between the samples and several paleo-environmental proxies, including the dinocyst *Operculodinium centrocarpum* from (Telesiński et al., 2024), ArW/meltwater indicator (%C37:4) (Łącka et al., 2019), and sea surface temperature (SST U_{37}^{K*}) (Łącka et al., 2019) (**Fig. S2**).

https://doi.org/10.5194/egusphere-2025-3780
Preprint. Discussion started: 18 August 2025

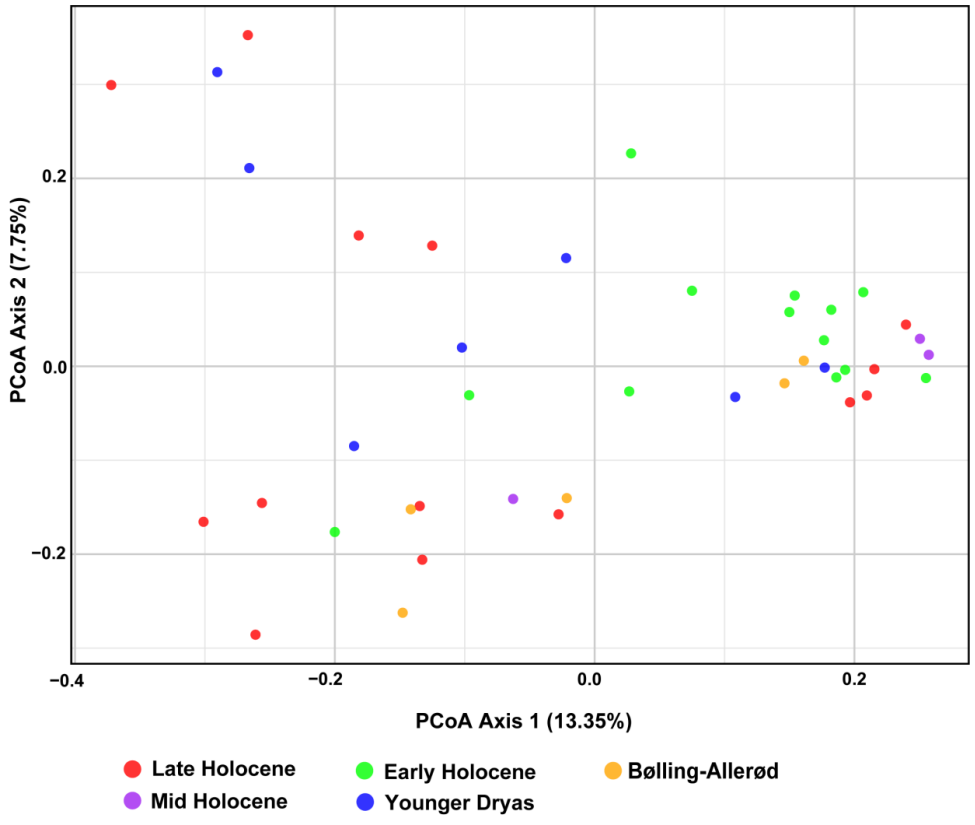

Figure 2. PcoA based on the Bray-Curtis dissimilarity matrix method with the eukaryote dataset (raw data converted into CSSlog1p formation).

4.4 Community composition

Within the dataset, a total of 236 ASVs were assigned to 14 Sub-Divisions, while 37 ASVs remained unassigned (**Table S2**). The Cercozoa was the most abundant sub-division, comprising 67 ASVs, accounting for 24.54% of the total ASVs (**Fig. 3 & Table S2**). Overall, the taxonomic structure of eukaryotes based on read abundance fluctuated significantly between samples (**Fig. 3a**). In contrast, ASV richness remained stable across different time periods except during the Bølling-Allerød period (**Fig.3b**). The number of unique ASVs was highest during the Late Holocene, with five unique ASVs identified. The Younger Dryas and Early Holocene each exhibited three unique ASVs. Conversely, no distinctive ASVs were identified during the Mid Holocene and Bølling–Allerød periods. Across the entire Holocene,

https://doi.org/10.5194/egusphere-2025-3780
Preprint. Discussion started: 18 August 2025

248 a total of 52 unique ASVs were recorded (**Fig.3b**).

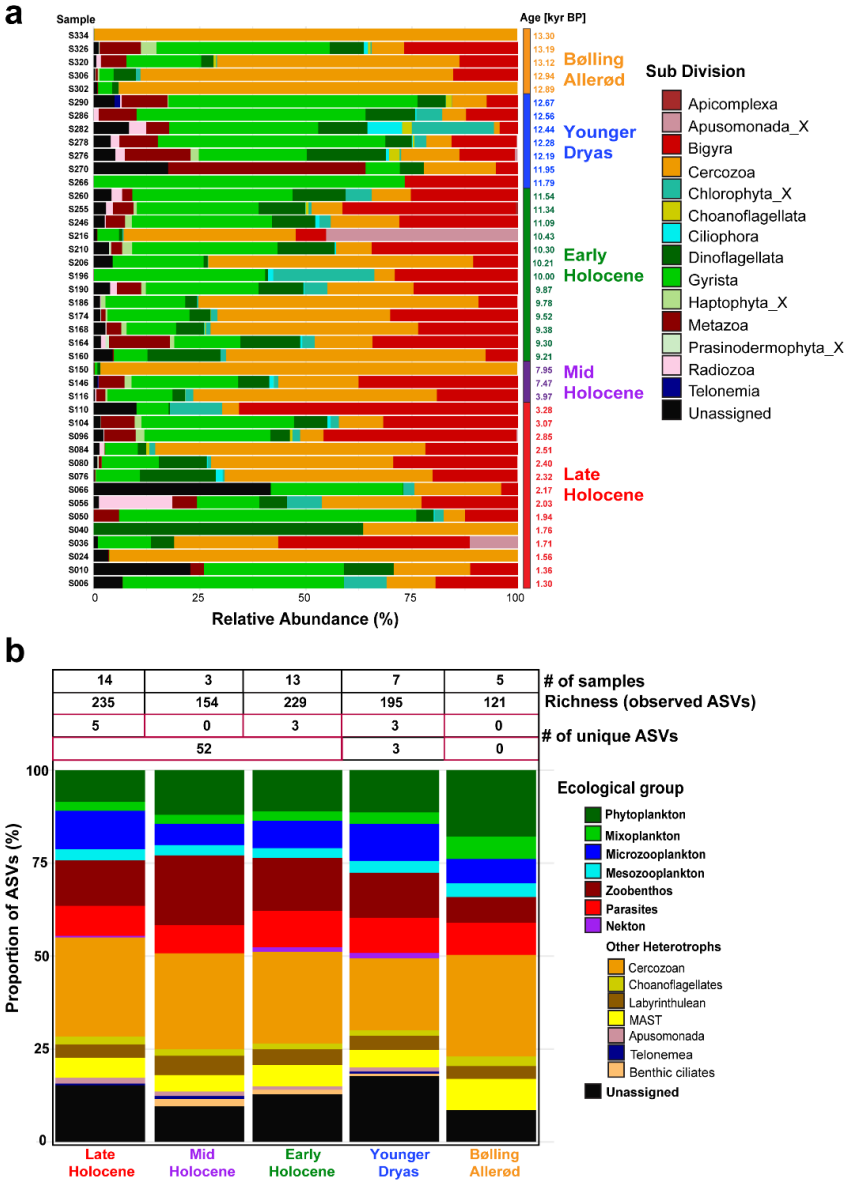

249

250 **Figure 3:** (a) Bar plot showing the downcore distribution of eukaryotic sub-divisions based on
251 their relative abundance. (b) Proportional richness of distinct ecological groups across selected
252 time periods (Bølling-Allerød, Younger Dryas, Early Holocene, Mid Holocene, and Late
253 Holocene), expressed as the percentage of ASVs. The accompanying table provides the number
254 of samples, the total number of observed ASVs and unique ASVs within each climate time
255 interval.

https://doi.org/10.5194/egusphere-2025-3780
Preprint. Discussion started: 18 August 2025

The ASVs were categorized based on their ecological roles, such as phytoplankton (31 ASVs), mixoplankton (8 ASVs), mesozooplankton (8 ASVs), microzooplankton (23 ASVs), parasites (24 ASVs), zoobenthos (36 ASVs), nekton (2 ASVs), and other heterotrophs (104 ASVs) (**Fig. 3b, Table S2**). The latter category comprises multiple taxonomic groups characterized by complex habitats and feeding behaviors, many of which have poorly understood ecological roles. This group includes Cercozoa (67 ASVs), Labyrinthulea (11 ASVs), Choanoflagellatea (5 ASVs), MAST (15 ASVs), benthic ciliophora (2 ASVs), Apusomonada (3 ASVs), and one ASV from the Telonemea flagellate group. The unassigned taxa (37 ASVs) also remained ecologically uncategorized. (**Fig. 3b**).

The phytoplankton community consisted of diatoms, green algae, haptophytes, and autotrophic dinoflagellates, most of which were associated with ArW (**Table S2**). In terms of read abundance, *Thalassiosira* spp. and *Chaetoceros* sp. dominated among diatoms, while *Micromonas polaris* was the dominant species within the green algae. The haptophytes group was primarily represented by *Phaeocytis* sp., whereas the *Gymnodinium* spp. and sea-ice-associated species *Polarella glacialis* were dominant within the autotrophic dinoflagellate group (**Fig. S3**). The mixoplankton community was primarily composed of mixotrophic dinoflagellates and silicoflagellates. In terms of read abundance, mixotrophic dinoflagellates were mainly present from the Younger Dryas to the beginning of the Early Holocene, whereas mixotrophic silicoflagellates, represented by *Pseudopedinella* sp., was present throughout the entire core (**Fig. S3**).

The zooplankton community was divided into two size-based groups: micro- and mesozooplankton. The microzooplankton group included heterotrophic protists such as radiolarians, pelagic ciliates, dinoflagellates, and silicoflagellates. These groups were identified as being present at specific time periods, e.g. ~12.4 to ~10.2 kyr, and ~2.3 to 1.3 kyr BP (**Fig. S4, Table S2**). The mesozooplankton group comprises small metazoans and was dominated by arthropods (Copepoda and Malacostraca) and larvaceans (Appendicularia). The copepod *Calanus* spp. represented the majority of the mesozooplankton around the study area (**Fig. S4**).

The zoobenthos was recorded as the most diverse group, primarily representing macrobenthic species. This group included annelids, ascidiacean, molluscs, cnidarians, and echinoderms (**Fig. S5, Table S2**). Zoobenthos taxa were most abundant around ~9.3 kyr BP, as well as between ~12.3 kyr and 12.0 kyr BP (**Fig. S5**).

The parasites were represented by six classes: Dinophyceae (Syndiniales), Gregarinomorphea, Paragregarea, Peronosporea, Hyphochytrea, and Enoplea (**Fig. S6, Table**

https://doi.org/10.5194/egusphere-2025-3780
Preprint. Discussion started: 18 August 2025

S2). Among them, Syndiniales have the highest abundance and diversity, with18 ASVs (mainly uncultured) detected throughout the studied time interval (**Fig. S6**). The nekton group included two ASVs assigned to Arctic cod (order Gnathostomata), which were detected only during the Younger Dryas and Early Holocene.

Among other heterotrophs, Cercozoa were dominant, accounting for a significant proportion of reads throughout the study period (**Fig. S7, Table S2**). Five classes of Cercozoa were identified: Ascetosporea, Phytomyxea, Granofilosea, Thecofilosea, and Imbricatea. Thecofilosea exhibited the highest richness with 51 ASVs (**Fig. S7, Table S2**). Ecologically, cercozoans can be classified as parasitic, predatory, and bacterivorous. *Cryothecomonas* spp. were identified as predatory, while those in the classes Ascetosporea and Phytomyxea were classified as parasites. Other cercozoan ASVs were identified only to the family level, limiting precise ecological interpretations.

The other heterotrophs also include the MAST (Marine Stramenopiles), Labyrinthulea, Choanoflagellata and Apusomonada. The MAST group included 16 ASVs, representing four main sub-clades: MAST-1, MAST-3, MAST-9, and MAST-12. MAST 9 and MAST 12 dominated throughout the studied time period and exhibited high richness (**Fig. S6, Table S2**).

The Labyrinthulea included saprotrophic Thraustochytriaceae, and Aplanochytriidae, revealing a dominant presence and high richness around ~11.8 kyr to ~2.2 kyr, and ~1.7 kyr BP (**Fig. 4**). Most choanoflagellate ASVs belonged to environmental clades, except for *Calliacantha* sp., which was dominated around ~12.7 kyr to ~12.2 kyr BP (**Fig. 4**). Apusomonada, represented by the class Apusomonadea, appeared during certain time intervals, especially the Early Holocene (~10.4 kyr BP), and Late Holocene (~1.7 kyr BP) (**Fig. 4, Table S2**). (see **Supplementary document** for more details).

https://doi.org/10.5194/egusphere-2025-3780
Preprint. Discussion started: 18 August 2025

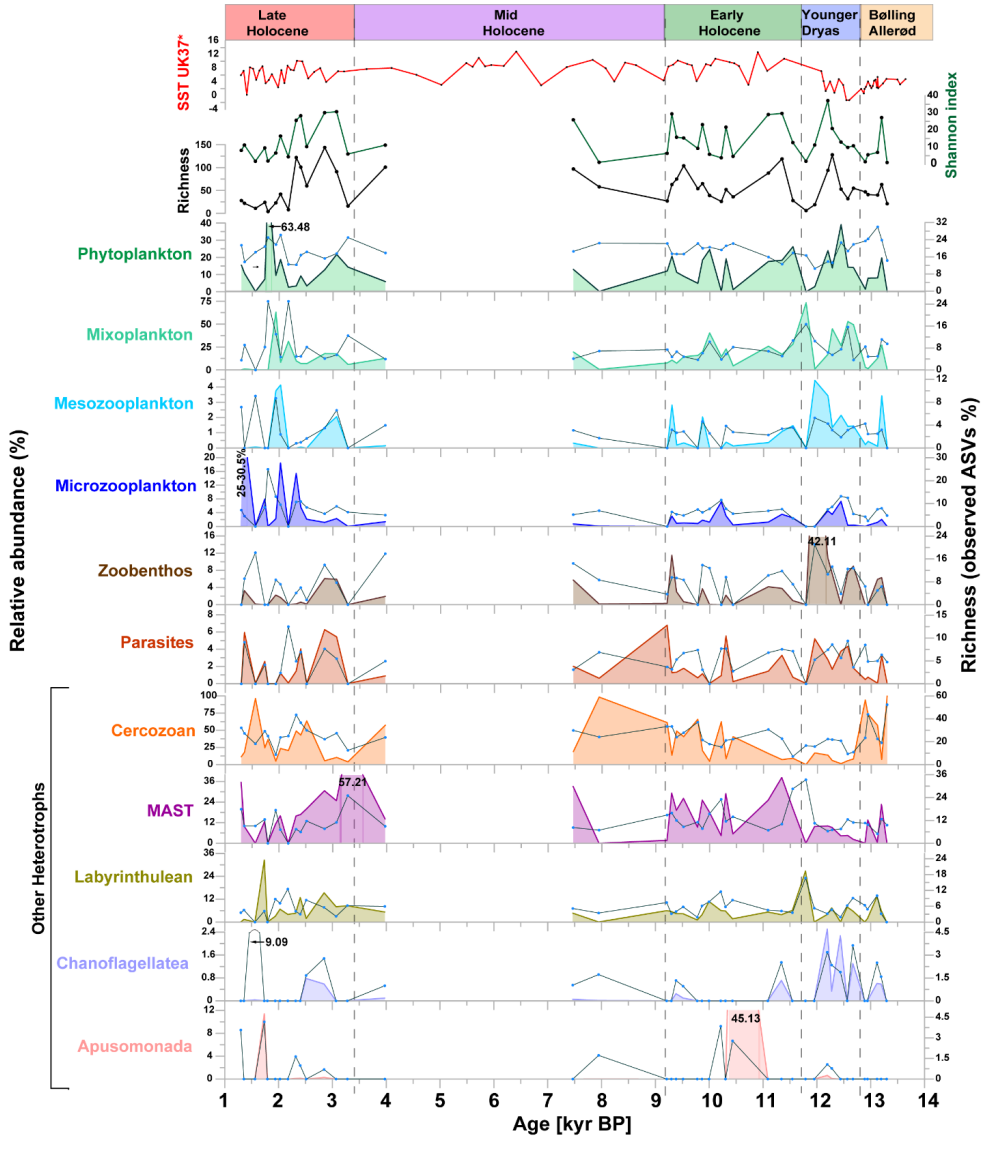

Figure 4: Relative abundance and richness (expressed as observed ASVs percentage) of major ecological groups, along with Shannon index, richness, and sea surface temperature [SST UK'37] from Łącka et al. [2019]. Lines represented ASVs abundance (%), and area represented the read abundance (%).

https://doi.org/10.5194/egusphere-2025-3780
Preprint. Discussion started: 18 August 2025

4.5 Indicator taxa for Arctic and Atlantic water conditions

A total of 39 ASVs were identified as potential indicator taxa using three analytical approaches (sPLS, Spearman correlation, and DESeq) (**Fig. S8, S9, Table S4**). Of these, 14 ASVs were identified as potential AW indicators, and belonged to the following groups: phytoplankton (1), microzooplankton (1), cercozoans (6), MAST (2), zoobenthos (1), labyrinthulean (1), and unassigned ASVs (2). The AW plankton indicators included a green algae *Pyramimonas* sp. (ASV55) and a pelagic ciliate *Cyclotrichium* sp. (ASV265), while the AW benthic indicators comprised a polychaete *Tharyx* sp. (ASV278) (**Fig. S10**).

In contrast, 24 ASVs were associated with ArW (**Fig. S12**), primarily parasites (5), zoobenthos (2), phytoplankton (3), choanoflagellates (2), microzooplankton (2), mesozooplankton (1), mixoplankton (1), benthic ciliate (1), nekton (1), and unassigned ASVs (6 s) (**Table S4**). Potential ArW ASV-based indicators were identified among both planktonic and benthic taxa. Planktonic ASVs comprised autotrophic dinoflagellates (*Prorocentrum* sp., ASV64 and ASV153), diatoms (*Chaetoceros gelidus*, ASV18), mixotrophic dinoflagellate (*Heterocapsa* sp., ASV204), pelagic ciliate (*Strombidium* sp., ASV123), radiolarian (*Heteracon* sp., ASV54), and mesozooplankton *(Oikopleura* sp., ASV500). Parasites included three Syndiniales dinoflagellates (ASV213, ASV341, and ASV391) and apicomplexan (*Paralecudina* sp., ASV958). Benthic indicators included benthic ciliate (*Holosticha* sp., ASV87), echinoderm (*Ctenodiscus* sp., ASV104), and bivalve (*Tridonta* sp., ASV137) (**Fig. S11**).

4.6 Ecological interactions among eukaryote families

Spearman correlation analysis ($r > 0.5$, adjusted $p < 0.001$) was used to explore potential ecological interactions among eukaryotic families inhabiting similar environmental niches (**Fig. S12, Table S5**). Parasitic cercozoans (Ascetosporea and Phagomyxidae) strongly correlated with algae families (Phaeocystaceae, Thalassiosiraceae, Pyramimonadaceae, and Prasinodermataceae), and dinoflagellates (Suessiaceae, and Gymnodiniaceae). Other cercozoans (CCW10-lineage, Novel-Clade-2, Cryothecomonas-lineage, and Ventricleftida) revealed significant correlations with algal and dinoflagellate groups (**Fig. S12, Table S5**). Among MAST groups, MAST-12 showed positive associations with algae families (Prasinodermataceae, Thalassiosiraceae, and Chaetocerotaceae) and parasites (Pirsoniaceae), while MAST-9 correlated with multiple phytoplankton families (**Fig. S12, Table S5**). Parasitic dinoflagellates (dino-group-II) showed strong correlation with haptophyte algae (Phaeocystaceae), diatom (Thalassiosiraceae), and dinoflagellates (Suessiaceae, and

https://doi.org/10.5194/egusphere-2025-3780
Preprint. Discussion started: 18 August 2025

Gymnodiniaceae). Parasitic alveolates of the family Lecudinidae showed a strong positive correlation with the mesozooplankton (Malacostraca), radiolarians and ophiuroids (**Fig. S12, Table S5**). Another parasitic superfamily of Stramenopiles, the Pirsoniaceae displayed strong associations with various taxa, including MAST-12, cercozoans (Thaumatomonadidae), green algae (Prasinodermataceae, and Chlamydomonadales), haptophytes (Phaeocystaceae), diatoms (Thalassiosiraceae), silicoflagellates (Actinomonadaceae), dinoflagelletes (Amphidiniopsidaceae), and polychaetae (Chaetopteridae) (**Fig.S12, Table S5**).

5. Discussion

This study expands our knowledge of eukaryotic communities' dynamics in the Storfjordrenna over the past 13,300 years by providing high-resolution sedaDNA records of both fossilized and non-fossilized groups. We demonstrate how these communities responded to major climatic shifts since the Bølling-Allerød and highlight key ecological interactions among major taxonomic groups. These findings enhance our understanding of how environmental changes have shaped eukaryotic biodiversity in southern Svalbard.

5.1.Impacts of climate change on the eukaryotic community in Storfjordrenna

5.1.1 Bølling-Allerød (13.30 kyr BP to 12.80 kyr BP)

The eukaryotic community in our record during the Bølling–Allerød reflected oceanographic conditions resembling those observed today in glacier-proximal areas of Arctic fjords characterized by high turbidity due to meltwater discharge and the presence of colder, fresher waters (Zajaczkowski, 2008; Łącka et al., 2019). Previous studies support this interpretation: the grounding line of the Svalbard Barents Ice Sheet (SBIS) retreated from Storfjordrenna before 13.95 kyr BP (Łącka et al., 2015), coinciding with SST reaching modern-like values (Łącka et al., 2019). However, despite elevated SST, primary productivity remained low—likely due to the suppressive effect of turbid meltwater input from the retreating ice sheet (Łącka et al., 2015). Biomarker data further indicated a dominance of fresher ArW over AW, which has been linked to reduced primary productivity (Łącka et al., 2019). These conditions favored the development of a eukaryotic community dominated by heterotrophs, capable of thriving in such extreme environments. The most abundant taxa, in terms of both sequence reads and ASV richness, were bacterivorous cercozoans (**Fig. 3**). The dominant cercozoan was *Limnofila* sp., a genus primarily found in fresh and brackish waters (Mylnikov et al., 2015; Nikolaev et al., 2003). Other important bacterivorous heterotrophs were MAST, particularly

https://doi.org/10.5194/egusphere-2025-3780
Preprint. Discussion started: 18 August 2025

MAST-9D and MAST-12A, known for their adaptation to extreme environmental conditions (Labarre et al., 2021; Lin et al., 2022; Obiol et al., 2024).

Despite lower read abundance, phytoplankton, mixoplankton, and microzooplankton showed high ASV richness during this period (**Fig. 3**). The phytoplankton community was dominated by autotrophic, sea-ice associated taxa, such as dinoflagellates *Polarella glacialis* (Harðardóttir et al., 2024) and *Gymnodinium* spp. (Kubiszyn and Wiktor, 2015), and diatom *Thalassiosira* spp. (Luddington et al., 2016). The mixoplankton was represented by the silicoflagellate, *Pseudopedinella elastica* (**Fig. S3**), which has been described as bacterivorous under conditions of limited light and nutrients (Gerea et al., 2016). The mesozooplankton community was primarily composed of herbivorous *Calanus* spp. and the omnivorous *Metridia longa*. These species have been observed in the Svalbard region in the present environment, with *Calanus* spp. dominating the ArW-AW in terms of biomass (Daase et al., 2008). Despite unfavorable conditions caused by meltwater influx and low nutrient availability, both primary and secondary productivity persisted, likely concentrated in ice-proximal and frontal zones where the stratification enhanced nutrient retention and water column stability. This suggests that environments near retreating ice sheets can act as biological hotspots, supporting productivity through ice-associated blooms and complex microbial food web interactions.

5.1.2 Younger Dryas (12.80 kyr BP to 11.70 kyr BP)

The eukaryotic community during the Younger Dryas reflected the dramatic environmental changes that occurred at that time. The most notable change was the rapid decrease in biodiversity during the Bølling-Allerød and Younger Dryas transition, when alpha diversity indices reached near-zero values (**Fig. 4**). It is most likely that the reorganization of oceanographic conditions caused a temporary slowdown of Atlantic meridional overturning circulation (AMOC) and a reduction in AW inflow leading to strong stratification, formation of perennial ice cover, and anoxic conditions at the bottom (Łącka et al., 2020). The presence of perennial ice cover led to a significant reduction in primary productivity in Storfjordrenna (Łącka et al., 2019). In contrast, the sedaDNA record also revealed the presence of phyto- and mixoplankton during this period, especially presence of phytoplankton *Thalassiosira* spp. and *Gymnodinium* sp., and silicoflagellate *P. elastica*, suggesting that primary productivity, yet limited, still occurred under the ice. The detection of herbivorous mesozooplankton *Calanus* spp., and predatory *Cryothecomonas* spp., also coincided with the presence of the phytoplankton community. Notably, the early Younger Dryas also revealed a short-term

https://doi.org/10.5194/egusphere-2025-3780
Preprint. Discussion started: 18 August 2025

increase in the relative abundance and diversity of zoobenthos, primarily polychaetae (*Barantolla* sp.) and molluscs (*Tridonta* sp. and *Talochlamys* sp.) (**Fig. S4**).

During the latter part of the Younger Dryas (after ~12.4 kyr BP), increasing advection of AW and SST warming led to the replacement of perennial sea ice by seasonal ice cover (Łącka et al., 2019; Łącka et al., 2020). This shift was followed by the establishment of a more diverse benthic foraminifera community (Łącka et al., 2015). Similarly, the sedaDNA record displayed the increase in the richness and abundance of zoobenthic taxa, mainly annelids, molluscs, and echinoderms (**Fig. S5**). However, the alkenone record suggested that the warming was associated with low primary productivity, probably due to the continuous input of turbid meltwater from the decaying SBIS (Łącka et al., 2015).

In contrast, the sedaDNA record indicated a sudden phytoplankton bloom in the latter Younger Dryas, dominated by *M. polaris, Thalassiosira* spp., *Chaetoceros gelidus*, and *Gymnodinium* spp. *Micromonas polaris* is typically associated with Arctic sea-ice environments, and favorably adapted to increasing Arctic temperatures and water column stratification (Grant et al., 2024). *Chaetoceros gelidus*, known for its high tolerance under variable light and ocean acidification conditions (Biswas, 2022; Ribeiro et al., 2024), may play a key role in plankton blooms and primary productivity, particularly during the Younger Dryas (**Fig. S3**). Phytoplankton blooms stimulated the development of secondary producers, mainly pelagic ciliates, and radiolarians, as well as mesozooplankton copepods (*Calanus* spp.) (**Fig. S4**). Altogether, these findings indicate that the latter part of the Younger Dryas (after ~12.4 kyr BP) was associated with periods of accelerated AW inflow and an increase in SST (Risebrobakken et al., 2010; Wollenburg et al., 2004), promoting phytoplankton and zooplankton growth, and enhancing benthic community development..

5.1.3 Early Holocene (11.70 kyr BP to 9.20 kyr BP)

The transition from the Younger Dryas to the Early Holocene was characterized by a significant drop in biodiversity and the dominance of mixoplankton, primarily *P. elastica*, as well as mixotrophic dinoflagellates such as *Biecheleria* sp. and *Gotoius* sp. According to (Łącka et al., 2020), the onset of the Early Holocene was associated with a short-term decrease in SST and a decrease in foraminiferal fauna abundance. The low biodiversity and dominance of mixotrophic plankton observed in the sedaDNA record might be a consequence of this short-term deterioration in environmental conditions.

However, the further development of the Early Holocene was driven by an increasing influence of AW in the area, which was followed by an increase in SST and productivity

https://doi.org/10.5194/egusphere-2025-3780
Preprint. Discussion started: 18 August 2025

(Devendra et al., 2023; Telesiński et al., 2017). Moreover, Arctic Front was located close to the Spitsbergen coast, leading to the formation of a highly productive frontal zone (Łącka et al., 2019). The amelioration of environmental conditions during the Early Holocene (Łącka et al., 2015) was reflected in a sudden peak of alpha diversity of overall eukaryotic community, accompanied by a notable increase in the richness and abundance of key ecological groups, including phytoplankton, zoobenthos, parasites, and other heterotrophs such as cercozoans and MAST. (**Fig. 4**). However, taxa associated with sea-ice were an important component of the assemblage, suggesting that sea-ice formation still occurred in Storfjordrenna. Despite AW dominance, the presence of a cercozoan *Limnofila* sp., green algae *M. polaris* and *Pyramimonas* sp., as well as sea-ice-indicator *P. glacialis* may suggest episodic presence of sea-ice, and transition of Arctic Front (**Fig. S3, S7**). Overall high eukaryotic biodiversity in the Early Holocene, particularly the diversity of phytoplankton, mixoplankton, mesozooplankton, and the gradual increase in MAST-9 species related to warm water further support the establishment of warm-water conditions with high nutrient availability (Łącka et al., 2019) (**Fig S3,S4, S6, and Table S4**).

5.1.4 Mid Holocene (9.20 kyr BP to 3.40 kyr BP)

Due to the lack of data from the period between 7.5 kyr BP and 4 kyr BP (see the Results section), it is possible to interpret only the early part of the Mid Holocene and the transition to the late Holocene. Therefore, this interpretation should be treated with caution due to the limited number of samples analyzed in this interval. The beginning of the Mid Holocene (9.2 kyr BP) in Storfjordrenna was marked by a significant drop in biodiversity, followed by an increase after 8.0 kyr BP. The species composition was predominantly composed of cercozoans, mainly *Limnofila* sp. and *Cryothecomonas* spp. (**Fig. S7**). Another important component of the eukaryotic assemblage was MAST species, including MAST-9D and MAST-12B, which had previously been recorded in the north Atlantic region (Lopez-Garcia et al., 2007; Newbold et al., 2012)(**Fig. S6**). The community composition resembled the one from Bølling Allerød, dominated by heterotrophic taxa adapted to extreme environmental conditions. This aligns with evidence of a minor cooling event between 9.0 kyr and 8.0 kyr BP, as proposed in prior studies (Łącka et al., 2015).

In contrast, despite their relatively low abundance, phytoplankton, mesozooplankton, and microzooplankton communities displayed relatively high diversity in the early Mid-Holocene. This period in Storfjordrenna was characterized by limited ice rafting, variable SST, and interplay between the AW and ArW water masses rather than a continuous impact of AW

https://doi.org/10.5194/egusphere-2025-3780
Preprint. Discussion started: 18 August 2025

(Łącka et al., 2019; Łącka et al., 2015). Furthermore, the low alkenone flux suggested low primary productivity throughout the mid-Holocene (Łącka et al., 2019), consistent with the low abundance of both phyto- and zooplankton taxa in the sedaDNA record. Low productivity was also observed at that time in the Norwegian and Svalbard shelves, potentially due to the limited nutrient availability. According to (Łącka et al., 2019), the reduction in primary productivity resulted from enhanced vertical stratification, which reduced vertical mixing in the water column, and thus, limited the nutrient resuspension to the surface. An alternative explanation is the early spring bloom, that occurs in the ice-free waters, and the subsequent development of mesozooplankton that graze on phytoplankton, thereby reducing the flux of organic matter to the bottom. However, the low abundance of sequences assigned to both phyto- and microzooplankton, as well as the increase in bacterivorous taxa, likely supports the first scenario. Overall, the lack of sea ice, and the variability in water masses and SST observed at the beginning of the Mid Holocene, created an unstable environment, which favored tolerant heterotrophic eukaryotes such as Cercozoans or MAST.

5.1.5 Late Holocene (3.40 kyr BP to 1.30 kyr BP)

The onset of the Late Holocene was marked by an increase in eukaryotic biodiversity, followed by a sharp decrease around 2.0 kyr BP. At this time, eukaryotic communities were predominantly composed of cercozoan and MAST (**Fig. 4**). Cercozoan abundance and richness exhibited an increasing, yet variable trend throughout the Late Holocene, whereas MAST decreased progressively over time.

Both phyto- and microzooplankton exhibited high richness, but variable abundance throughout the Late Holocene (**Fig. 4**). Furthermore, the presence of parasitic species, including the Syndiniales dinoflagellate (dino-group-I and dino-group-II) as well as the diatom-associated parasitic *Pirsonia* sp., co-occurred with the phytoplankton suggesting that parasitic interactions may have influenced phytoplankton dynamics during the Late Holocene. (**Fig. S12, Table S5**). The Late Holocene coincided with the so-called Neoglacial cooling, spanning the last 4.0 kyr BP. This period was characterized by a decline in SST (Risebrobakken et al., 2010), limited AW inflow and strengthening of ArW flow, which led to the formation of extensive ice cover (Martrat et al., 2003; Berben et al., 2014; Devendra et al., 2023). Records from Storfjordrenna also showed a cooling in the area, associated with enhanced ice rafting (Łącka et al., 2019; Łącka et al., 2015). Thus, the increased abundance of phytoplankton in general, and ice-associated *P. glacialis* in particular, is probably an effect of the cooling of surface waters and the formation of sea-ice, which launched convective water mixing and

https://doi.org/10.5194/egusphere-2025-3780
Preprint. Discussion started: 18 August 2025

nutrient resuspension to the surface. In consequence, primary productivity increased, stimulating the development of the microzooplankton community (**Fig. S4**).

5.2. SedaDNA environmental indicators

This study identified 39 potential eukaryotic indicator taxa associated with AW and ArW conditions. Several taxa exhibited consistent temporal patterns that aligned with paleoenvironmental proxies, supporting their potential for long-term reconstructions. In contrast, others appeared only sporadically, reducing their reliability as potential indicators. AW-associated taxa were primarily represented by cercozoans and MAST, while ArW-associated taxa included diatoms, dinoflagellates, choanoflagellates, Arctic zoobenthos, and zooplankton.

Bacterivorous cercozoans, including the Ventricleftida (ASV46), the Protaspa-lineage (ASV83, ASV623, and ASV257), and the CCW10-lineage (ASV20), were identified as potential indicators for the AW (**Table S4**). However, their identification is currently based exclusively on molecular data, limiting ecological and biogeographical context and weakening their use in environmental reconstructions (Labarre et al., 2021; Obiol et al., 2024). Similarly, members of the bacterivorous MAST-9 group, notably MAST-9A and MAST-9D, were exclusively detected in AW conditions (**Fig. S10, Table S4**), consistent with their known tropical-to-temperate distribution. Within the phytoplankton communities, *Pyramimonas parkeae* (a green alga that prefers higher temperature regions; (Bock et al., 2021)), and the microzooplankton pelagic ciliate *Cyclotrichium* sp. (commonly found in warmer waters; (Dirmenci et al., 2010; Xu et al., 2005)) were also identified as potential AW indicators. However, they only occurred in a brief temporal window near the end of the Early Holocene, so their reliability as indicators needs to be verified by further studies (**Fig. S10**).

The relatively high number of cold-water species recorded was probably due to favorable overall conditions in the study area. The autotrophic *Prorocentrum* spp. are known as toxin-producing, bloom-forming species with broad global distributions, including polar regions (Cen et al., 2019; Goncharenko et al., 2021; Stoecker and Lavrentyev, 2018; Tillmann et al., 2022). In the present study, both taxa were primarily detected at the onset of the Younger Dryas (**Table S5**). Their limited distribution suggests that they may be constrained as long-term environmental indicators. Similarly, *Heterocapsa* sp., a mixotrophic dinoflagellate commonly associated with harmful algal blooms in Arctic and North Atlantic waters (Wu et al., 2022; Rintala et al., 2010), was identified as a potential ArW indicator. The genus *Holosticha* is a widespread benthic ciliate, associated with sea ice (Berger, 2003; Wilbert and Song, 2008; Petz

https://doi.org/10.5194/egusphere-2025-3780
Preprint. Discussion started: 18 August 2025

et al., 1995), and known to feed on diatoms and flagellates (Lei et al., 2005), which was also identified as a potential ArW indicator. However, their presence was confined to the Bølling-Allerød and Younger Dryas or the Younger Dryas and Early Holocene intervals, respectively, limiting their reliability as a long-term proxy for ArW conditions (**Fig. S11**).

In contrast, the ArW-associated diatom species *Chaetoceros gelidus* was consistently abundant, (**Fig. S12**), contributing to bloom formation and demonstrating adaptability to low light conditions (Hoppe et al., 2018; Biswas, 2022). Among the zooplankton, two taxa were identified as potential indicators: the microzooplankton radiolarian species *Heteracon* sp. and the mesozooplankton filter feeder appendicularian *Oikopleura vanhoeffeni* (Deibel, 1986, 1988) (Fig. S12). Likewise, the cold-water bivalve species *Tridonta* sp. which is commonly found in the North Atlantic and Arctic region (Marincovich et al., 2002; Petersen, 2001), demonstrated strong potential as an indicator species. Within parasitic dinoflagellates, two potential indicators belonging to dino-group-I, mostly associated with sea-ice conditions (Clarke et al., 2019), were identified. Choanoflagellate recorded in the study can be identified as a sea-ice associated group due to the presence of two potential ArW indicator taxa (Buck and Garrison, 1988; Thomsen and Ostergaard, 2017). These taxa were all consistently present throughout the study period, suggesting a stable association with cold marine conditions.

Chaetoceros gelidus, Oikopleura vanhoeffeni, Calliacantha sp. and *Tridonta* sp. demonstrated the greatest indicative potential, with consistent presence and alignment with multiple paleo proxies (**Table S4**). However, their Spearman correlation coefficients between environmental variables ranged from 0.3 to 0.5 ($p < 0.05$), indicating a weak to moderate association. This may be due to a combination of interspecific competition and the influence of multiple external environmental variables in the study area. These interacting factors contribute to the complexity of the ecosystem and limit the effectiveness of using single-proxy approaches when interpreting the responses of indicator species in paleoenvironmental reconstructions. Further studies of eukaryotic communities in other Arctic regions are therefore needed to validate these taxa as robust indicator species.

5.3. Interactions within eukaryotic community structure in Storfjordrenna

The biodiversity of eukaryotic communities in Storfjordrenna was previously influenced by the interplay between ArW and AW masses, as well as sea-ice coverage over the past 13.30 kyr BP. Throughout the study period, eukaryotic biodiversity remained relatively stable, with a notable exception during the transitions between major climatic intervals (**Fig. 3**). Peaks of

https://doi.org/10.5194/egusphere-2025-3780
Preprint. Discussion started: 18 August 2025

biodiversity coincided with the presence of sea-ice margins and frontal zones, environments known to promote phytoplankton growth and primary productivity (**Fig. 4**).

Analysis of phytoplankton diversity revealed a consistent presence of green algae throughout the study period, except during the Bølling Allerød interstadial, when diatoms dominated. Taxonomic abundance showed dynamic fluctuations, with gradual declines observed during the transitions between major climatic intervals. This suggests that environmental instability may have influenced the structure of the phytoplankton community.

Key contributors to primary productivity in the Storfjordrenna included diatoms (*Thalassiosira* spp., and *Chaetoceros* spp.), green algae (*M. polaris*), and autotrophic dinoflagellates (*P. glacialis*, and *Gymnodinium* spp.). Additionally, Spearman rank correlation analysis showed that the family Actinomonadaceae, mainly represented by *Pseudopedinella* sp., was positively associated with diatoms. Spearman rank correlation analysis also revealed a strong positive association between parasitic cercozoans and phytoplankton communities (**Table S5**), indicating that the presence of parasitic cercozoans may play a significant role in shaping ecological interactions within phytoplankton assemblages (Bass et al., 2009; Cavalier-Smith and Chao, 2003; Hartikainen et al., 2014). Conversely, the parasitic apicomplexan family Lecudinidae exhibited a robust association with zoobenthos (e.g., Heteroconchia and Ophiurida) and mesozooplankton (e.g., Malacostraca), highlighting their parasitic relationships with marine invertebrates (Rueckert et al., 2015). Parasitic dinoflagellates (dino-group-II) maintained a positive association with haptophytes and diatoms. The parasitic nanoflagellate Pirsoniaceae: *Pirsonia* sp., demonstrated a strong correlation with autotrophic microbes, including, dinoflagellates, diatoms, and silicoflagellates. (Kuhn et al., 2004; Schweikert and Schnepf, 1997). This raises questions about the nature of their ecological interactions, and whether they are strictly parasitic or co-occur under similar environmental conditions. These findings emphasize the need for further investigation to understand the mechanisms driving these interactions and their broader implications for microbial community dynamics.

Cercozoans have emerged as the most dominant group within the eukaryotic community, in terms of both abundance and species richness. Cercozoan community included taxa previously recorded in various habitats including fresh and marine environments (Chantangsi and Leander, 2010; Irwin et al., 2019). Their occurrence across a wide range of environmental conditions highlights their ecological flexibility and broad tolerance. Although cercozoans as a group exhibit high richness, only a few lineages, such as the Imbricata-novel clade 2, *Protaspa* spp., *Cryothecomonas* spp., and Ascetosporea, persisted consistently throughout the study period,

https://doi.org/10.5194/egusphere-2025-3780
Preprint. Discussion started: 18 August 2025

while most of the others were restricted to specific time intervals (**Fig. S7**). This suggests that, although cercozoans as a whole group may not showed sensitivity to environmental shifts, individual lineages are likely to be more responsive.

MAST species also constituted a major microbial group within the eukaryotic community, with MAST-9 dominant overall and MAST-12 particularly prevalent during the late Holocene. These two MAST subgroups are commonly associated with temperate regions or extreme environments such as cold seeps (Lin et al., 2022; Obiol et al., 2024). The statistical analysis identified potential warm-water indicator species within these groups (**Fig. S10, Table S4**). Based on the co-occurrence relation, the MAST-12, and MAST-9 subgroup revealed a strong correlation (> 0.6) with the parasitic family of Pirsoniaceae and the phytoplankton families (**Table S5**), providing insight into their ecological activities within the eukaryotic community. Further analysis of the ecological traits and distribution of micro eukaryotic taxa, mainly cercozoans and MAST, could provide deeper insights into their ecological responses within the Storfjordrenna ecosystem.

6. Conclusions

Using sedaDNA metabarcoding, we reconstructed the paleoecology of eukaryotic communities in Storfjordrenna over the last 13.30 kyr BP, elucidating their sensitivity and adaptability to environmental variables. Overall, the eukaryotic biodiversity in Storfjordrenna remained relatively stable, with a notable exception during the transitions between major climatic intervals. Peaks of biodiversity coincided with the presence of sea-ice margins and frontal zones, environments known to foster favorable conditions for phytoplankton development. Cercozoans and MAST emerged as dominant groups, highlighting their ecological flexibility and broad tolerance. This study revealed that primary productivity in the Storfjordrenna region over the investigated time period was mainly driven by phytoplankton, including diatoms (*Thalassiosira* spp., *Chaetoceros* spp.), green algae (*Micromonas* spp.), and autotrophs dinoflagellates (*P. glacialis*,) as well as mixoplankton species such as *Pseudopedinella elastica*. Several potential ASV-indicators were identified through multi-method analyses, including taxa associated with specific water masses. Our findings also underscore the complex interplay of environmental drivers shaping community composition, revealing both positive and negative associations among key microbial taxa. Our findings highlight the potential of sedaDNA for reconstructing past eukaryotic communities and detecting environmental change. However, improving taxonomic resolution and validating

https://doi.org/10.5194/egusphere-2025-3780
Preprint. Discussion started: 18 August 2025

indicator taxa remain essential for establishing robust palaeoecological indicators in Storfjordrenna and the broader Svalbard region.

Data availability. Raw reads of 18S-V1V2 rDNA sequencing generated in this study were deposited in the National Center for Biotechnology Information (NCBI) under Bio Project PRJNA1299363, and the remaining data and additional details used for this study can be found in the Supplement tables (Table S1-S5), Supplementary figures (S1-S12), and Supplementary document.

Supplement. The supplement related to this article is available online at XXX.

Author contributions. HN and Joanna **P,** designed the study. Joanna **P** extract the DNA. **HN** analyzed the DNA data, and performed bioinformatic, statistical analyses, and interpret the results. Joanna **P,** Jan **P** and **N-LN** helped with the bioinformatic analysis, and interpret the results. **MŁ** and **DD** help to clarify the age depth model, and the paleoenvironmental data. **HN** drafted the paper, and prepared the figures, and tables. All authors contributed to data interpretation and writing of the manuscript.

Competing interests. The contact author has declared that none of the authors has any competing interests.

Acknowledgements. We thank the captain and crew of R/V Jan Mayen, as well as the cruise participants, in particular Steinar Iversen, for their help at sea.

Financial support. The research was financially supported by the National Science Centre in Poland through project 2022/47/B/ST10/03050.

7. Reference

Armbrecht, L. H.: The potential of sedimentary Ancient DNA to reconstruct past ocean ecosystems, Oceanography, 33, 116-123, https://doi.org/10.5670/oceanog.2020.211, 2020.

Årthun, M., Eldevik, T., Smedsrud, L. H., Skagseth, Ø., and Ingvaldsen, R. B.: Quantifying the influence of Atlantic heat on Barents sea ice variability and retreat, J. Clim., 25, 4736-4743, https://doi.org/10.1175/jcli-d-11-00466.1, 2012.

Bass, D., Chao, E. E., Nikolaev, S., Yabuki, A., Ishida, K., Berney, C., Pakzad, U., Wylezich, C., and Cavalier-Smith, T.: Phylogeny of novel naked Filose and Reticulose Cercozoa: Granofilosea cl. n. and Proteomyxidea revised, Protist, 160, 75-109, https://doi.org/10.1016/j.protis.2008.07.002, 2009.

Benner, I., Irwin, A. J., and Finkel, Z. V.: Capacity of the common Arctic picoeukaryote Micromonas to adapt to a warming ocean, Limnol. Oceanogr. Lett., 5, 221-227, https://doi.org/10.1002/lol2.10133, 2019.

https://doi.org/10.5194/egusphere-2025-3780
Preprint. Discussion started: 18 August 2025

677 Bensi, M., Nilsen, F., Ferré, B., Skogseth, R. E., Moskalik, M., Korhonen, M., Vogedes, D. L.,
678 Kovacevic, V., Paladini de Mendoza, F., and Ingrosso, G.: The Atlantification process in Svalbard: a
679 broad view from the SIOS Marine Infrastructure network (ARiS), SIOS, 138-151,
680 https://doi.org/10.5281/zenodo.14425672, 2025.

681 Berben, S. M. P., Husum, K., Cabedo-Sanz, P., and Belt, S. T.: Holocene sub-centennial evolution of
682 Atlantic water inflow and sea ice distribution in the western Barents Sea, Climate of the Past, 10, 181-
683 198, https://doi.org/10.5194/cp-10-181-2014, 2014.

684 Berger, H.: Redefinition of Holosticha Wrzesniowski, 1877 (Ciliophora, Hypotricha), Eur. J. Protistol.,
685 39, 373-379, https://doi.org/10.1078/0932-4739-00006, 2003.

686 Biswas, H.: A story of resilience: Arctic diatom Chaetoceros gelidus exhibited high physiological
687 plasticity to changing CO(2) and light levels, Front Plant Sci, 13, 1028544,
688 https://doi.org/10.3389/fpls.2022.1028544, 2022.

689 Blindheim, J. and Osterhus, S.: The Nordic Seas, main Oceanographic features American Geophysical
690 Union, 158, 11, https://doi.org/doi:10.1029/158GM03, 2005.

691 Bock, N. A., Charvet, S., Burns, J., Gyaltshen, Y., Rozenberg, A., Duhamel, S., and Kim, E.:
692 Experimental identification and in silico prediction of bacterivory in green algae, ISME J, 15, 1987-
693 2000, 10.1038/s41396-021-00899-w, 2021.

694 Buck, K. R. and Garrison, D. L.: Distribution and Abundance of Choanoflagellates (Acanthoecidae)
695 across the Ice-Edge Zone in the Weddell Sea, Antarctica, Mar. Biol., 98, 263-269,
696 https://doi.org/10.1007/Bf00391204, 1988.

697 Callahan, B. J., McMurdie, P. J., Rosen, M. J., Han, A. W., Johnson, A. J., and Holmes, S. P.: DADA2:
698 High resolution sample inference from amplicon data, Nat. Methods, 13, 581–583,
699 https://doi.org/10.1038/nmeth.3869, 2016.

700 Cavalier-Smith, T. and Chao, E. E.: Phylogeny and classification of phylum Cercozoa (Protozoa),
701 Protist, 154, 341-358, https://doi.org/10.1078/143446103322454112, 2003.

702 Cen, J., Wang, J., Huang, L., Ding, G., Qi, Y., Cao, R., Cui, L., and Lü, S.: Who is the “murderer” of
703 the bloom in coastal waters of Fujian, China, in 2019?, J. Oceanol. Limnol., 38, 722-732,
704 https://doi.org/10.1007/s00343-019-9178-6, 2019.

705 Chantangsi, C. and Leander, B. S.: An SSU rDNA barcoding approach to the diversity of marine
706 interstitial cercozoans, including descriptions of four novel genera and nine novel species, Int. J. Syst.
707 Evol. Microbiol., 60, 1962-1977, https://doi.org/10.1099/ijs.0.013888-0, 2010.

708 Chao, A., Chiu, C.-H., and Jost, L.: Unifying Species Diversity, Phylogenetic Diversity, Functional
709 Diversity, and Related Similarity and Differentiation Measures Through Hill Numbers, Annu. Rev.
710 Ecol. Evol. Syst., 45, 297-324, https://doi.org/10.1146/annurev-ecolsys-120213-091540, 2014.

711 Clarke, L. J., Bestley, S., Bissett, A., and Deagle, B. E.: A globally distributed Syndiniales parasite
712 dominates the Southern Ocean micro-eukaryote community near the sea-ice edge, ISME J, 13, 734-
713 737, https://doi.org/10.1038/s41396-018-0306-7, 2019.

714 Daase, M., Eiane, K., Aksnes, D. L., and Vogedes, D.: Vertical distribution of Calanus spp. and Metridia
715 longa at four Arctic locations, Mar. Biol. Res., 4, 193-207,
716 https://doi.org/10.1080/17451000801907948, 2008.

717 Deb, J. C. and Bailey, S. A.: Arctic marine ecosystems face increasing climate stress, Environ. Rev., 31,
718 403-451, https://doi.org/10.1139/er-2022-0101, 2023.

719 Deibel, D.: Feeding mechanism and house of the Appendicularian Oikopleura-Vanhoeffeni, Mar. Biol.,
720 93, 429-436, https://doi.org/10.1007/Bf00401110, 1986.

https://doi.org/10.5194/egusphere-2025-3780
Preprint. Discussion started: 18 August 2025

721 Deibel, D.: Filter feeding by Oikopleura-Vanhoeffeni - Grazing impact on suspended particles in cold
722 Ocean Waters, Mar. Biol., 99, 177-186, https://doi.org/10.1007/Bf00391979, 1988.

723 Devendra, D., Łącka, M., Szymańska, N., Szymczak-Żyła, M., Krajewska, M., Weiner, A. K. M., De
724 Schepper, S., Simon, M. H., and Zajączkowski, M.: The development of ocean currents and the response
725 of the cryosphere on the Southwest Svalbard shelf over the Holocene, Global Planet. Change, 228,
726 10.1016/j.gloplacha.2023.104213, 2023.

727 Dirmenci, T., Dündar, E., Deniz, G., Arabaci, T., Martin, E., and Jamzad, Z.: Morphological,
728 karyological and phylogenetic evaluation of Cyclotrichium: a piece in the tribe Mentheae puzzle, Turk
729 J Bot, https://doi.org/10.3906/bot-0912-3, 2010.

730 Dufresne, Y., Lejzerowicz, F., Perret-Gentil, L. A., Pawlowski, J., and Cordier, T.: SLIM: a flexible web
731 application for the reproducible processing of environmental DNA metabarcoding data, BMC
732 Bioinformatics, 20, 88, https://doi.org/10.1186/s12859-019-2663-2, 2019.

733 Froslev, T. G., Kjoller, R., Bruun, H. H., Ejrnaes, R., Brunbjerg, A. K., Pietroni, C., and Hansen, A. J.:
734 Algorithm for post-clustering curation of DNA amplicon data yields reliable biodiversity estimates, Nat
735 Commun, 8, 1188, https://doi.org/10.1038/s41467-017-01312-x, 2017.

736 Gerea, M., Saad, J. F., Izaguirre, I., Queimaliños, C., Gasol, J. M., and Unrein, F.: Presence, abundance
737 and bacterivory of the mixotrophic algae Pseudopedinella (Dictyochophyceae) in freshwater
738 environments, Aquat. Microb. Ecol., 76, 219-232, https://doi.org/10.3354/ame01780, 2016.

739 Goncharenko, I., Krakhmalnyi, M., Velikova, V., Ascencio, E., and Krakhmalnyi, A.: Ecological niche
740 modeling of toxic dinoflagellate Prorocentrum cordatum in the Black Sea, Ecohydrology &
741 Hydrobiology, 21, 747-759, https://doi.org/10.1016/j.ecohyd.2021.05.002, 2021.

742 Górska, B., Gromisz, S., Legeżyńska, J., Soltwedel, T., and Włodarska-Kowalczuk, M.: Macrobenthic
743 diversity response to the atlantification of the Arctic Ocean (Fram Strait, 79°N) – A taxonomic and
744 functional trait approach, Ecol. Indic., 144, 109464, https://doi.org/10.1016/j.ecolind.2022.109464,
745 2022.

746 Grant, D. M., Steinsland, K., Cordier, T., Ninnemann, U. S., Ijaz, U. Z., Dahle, H., De Schepper, S., and
747 Ray, J. L.: Sedimentary ancient DNA sequences reveal marine ecosystem shifts and indicator taxa for
748 glacial-interglacial sea ice conditions, Quat. Sci. Rev., 339,
749 https://doi.org/10.1016/j.quascirev.2024.108619, 2024.

750 Guillou, L., Bachar, D., Audic, S., Bass, D., Berney, C., Bittner, L., Boutte, C., Burgaud, G., de Vargas,
751 C., Decelle, J., Del Campo, J., Dolan, J. R., Dunthorn, M., Edvardsen, B., Holzmann, M., Kooistra, W.
752 H., Lara, E., Le Bescot, N., Logares, R., Mahe, F., Massana, R., Montresor, M., Morard, R., Not, F.,
753 Pawlowski, J., Probert, I., Sauvadet, A. L., Siano, R., Stoeck, T., Vaulot, D., Zimmermann, P., and
754 Christen, R.: The Protist Ribosomal Reference database (PR2): a catalog of unicellular eukaryote small
755 sub-unit rRNA sequences with curated taxonomy, Nucleic Acids Res., 41, D597-604,
756 https://doi.org/10.1093/nar/gks1160, 2013.

757 Hallegraeff, G. M.: Ocean Climate Change, Phytoplankton community responses, and harmful algal
758 blooms: A formidable predictive challenge, J. Phycol., 46, 220-235, https://doi.org/10.1111/j.1529-
759 8817.2010.00815.x, 2010.

760 Harðardóttir, S., Haile, J. S., Ray, J. L., Limoges, A., Van Nieuwenhove, N., Lalande, C., Grondin, P.-
761 L., Jackson, R., Skaar, K. S., Heikkilä, M., Berge, J., Lundholm, N., Massé, G., Rysgaard, S.,
762 Seidenkrantz, M.-S., De Schepper, S., Lorenzen, E. D., Lovejoy, C., and Ribeiro, S.: Millennial-scale
763 variations in Arctic sea ice are recorded in sedimentary ancient DNA of the microalga Polarella glacialis,
764 Commun. Earth Environ., 5, https://doi.org/10.1038/s43247-023-01179-5, 2024.

765 Hartikainen, H., Ashford, O. S., Berney, C., Okamura, B., Feist, S. W., Baker-Austin, C., Stentiford, G.
766 D., and Bass, D.: Lineage-specific molecular probing reveals novel diversity and ecological partitioning
767 of haplosporidians, ISME J, 8, 177-186, https://doi.org/10.1038/ismej.2013.136, 2014.

https://doi.org/10.5194/egusphere-2025-3780
Preprint. Discussion started: 18 August 2025

768 Heaton, T. J., Köhler, P., Butzin, M., Bard, E., Reimer, R. W., Austin, W. E. N., Bronk Ramsey, C.,
769 Grootes, P. M., Hughen, K. A., Kromer, B., Reimer, P. J., Adkins, J., Burke, A., Cook, M. S., Olsen, J.,
770 and Skinner, L. C.: Marine20—The Marine Radiocarbon Age Calibration Curve (0–55,000 cal BP),
771 Radiocarbon, 62, 779-820, https://doi.org/10.1017/rdc.2020.68, 2020.

772 Hop, H., Wold, A., Vihtakari, M., Daase, M., Kwasniewski, S., Gluchowska, M., Lischka, S., Buchholz,
773 F., and Falk-Petersen, S.: Zooplankton in Kongsfjorden (1996–2016) in Relation to Climate Change,
774 in: The Ecosystem of Kongsfjorden, Svalbard, Advances in Polar Ecology, 229-300,
775 https://doi.org/10.1007/978-3-319-46425-1_7, 2019.

776 Hopkins, T. S.: The Gin Sea - a Synthesis of Its Physical Oceanography and Literature-Review 1972-
777 1985, Earth-Sci. Rev., 30, 175-318, https://doi.org/10.1016/0012-8252(91)90001-V, 1991.

778 Hoppe, C. J. M., Wolf, K. K. E., Schuback, N., Tortell, P. D., and Rost, B.: Compensation of ocean
779 acidification effects in Arctic phytoplankton assemblages, Nat. Clim. Change, 8, 529-533,
780 https://doi.org/10.1038/s41558-018-0142-9, 2018.

781 IPCC: Climate Change 2022: Impacts, Adaptation, and Vulnerability: Contribution of Working Group
782 II to the Sixth Assessment Report of the Intergovernmental Panel on Climate Change, Cambridge,
783 https://doi.org/10.1017/9781009325844, 2023.

784 Irwin, N. A. T., Tikhonenkov, D. V., Hehenberger, E., Mylnikov, A. P., Burki, F., and Keeling, P. J.:
785 Phylogenomics supports the monophyly of the Cercozoa, Mol. Phylogenet. Evol., 130, 416-423,
786 https://doi.org/10.1016/j.ympev.2018.09.004, 2019.

787 Kassambara, A.: ggpubr:'ggplot2'based publication ready plots [code], 2023.

788 Kim-Anh Lê Cao, Debra Rossow, Christèle Robert-Granié, and Besse, P.: A Sparse PLS for variable
789 selection when integrating Omics data, Stat. Appl. Genet. Mol. Biol., 7, 35, 2008.

790 Kruskal, W. H. and Wallis, W. A.: Use of ranks in one-criterion variance analysis, J. Am. Stat. Assoc.. ,
791 47, 583-621, 1952.

792 Kubiszyn, A. M. and Wiktor, J. M.: The Gymnodinium and Gyrodinium (Dinoflagellata:
793 Gymnodiniaceae) of the West Spitsbergen waters (1999–2010): biodiversity and morphological
794 description of unidentified species, Polar Biol., 39, 1739-1747, https://doi.org/10.1007/s00300-015-
795 1764-2, 2015.

796 Kuhn, S., Medlin, L., and Eller, G.: Phylogenetic position of the parasitoid nanoflagellate Pirsonia
797 inferred from nuclear-encoded small subunit ribosomal DNA and a description of Pseudopirsonia n.
798 gen. and Pseudopirsonia mucosa (Drebes) comb. nov, Protist, 155, 143-156,
799 https://doi.org/10.1078/143446104774199556, 2004.

800 Labarre, A., Lopez-Escardo, D., Latorre, F., Leonard, G., Bucchini, F., Obiol, A., Cruaud, C., Sieracki,
801 M. E., Jaillon, O., Wincker, P., Vandepoele, K., Logares, R., and Massana, R.: Comparative genomics
802 reveals new functional insights in uncultured MAST species, ISME J, 15, 1767-1781,
803 https://doi.org/10.1038/s41396-020-00885-8, 2021.

804 Łącka, M., Zajączkowski, M., Forwick, M., and Szczuciński, W.: Late Weichselian and Holocene
805 palaeoceanography of Storfjordrenna, southern Svalbard, Climate of the Past, 11, 587-603,
806 https://doi.org/10.5194/cp-11-587-2015, 2015.

807 Łącka, M., Cao, M., Rosell-Melé, A., Pawłowska, J., Kucharska, M., Forwick, M., and Zajączkowski,
808 M.: Postglacial paleoceanography of the western Barents Sea: Implications for alkenone-based sea
809 surface temperatures and primary productivity, Quat. Sci. Rev., 224,
810 https://doi.org/10.1016/j.quascirev.2019.105973, 2019.

811 Łącka, M., Michalska, D., Pawlowska, J., Szymanska, N., Szczucinski, W., Forwick, M., and
812 Zajaczkowski, M.: Multiproxy paleoceanographic study from the western Barents Sea reveals dramatic

https://doi.org/10.5194/egusphere-2025-3780
Preprint. Discussion started: 18 August 2025

Younger Dryas onset followed by oscillatory warming trend, Sci. Rep., 10, 15667, https://doi.org/10.1038/s41598-020-72747-4, 2020.

Lei, Y., Xu, K., and Choi, J. K.: Holosticha hamulata n. sp. and Holosticha heterofoissneri Hu and Song, 2001, two urostylid ciliates (protozoa, ciliophora) from intertidal sediments of the yellow sea, J. Eukaryot. Microbiol., 52, 310-318, https://doi.org/10.1111/j.1550-7408.2005.00039.x, 2005.

Lin, Y. C., Chin, C. P., Yang, J. W., Chiang, K. P., Hsieh, C. H., Gong, G. C., Shih, C. Y., and Chen, S. Y.: How communities of Marine Stramenopiles varied with environmental and biological variables in the subtropical northwestern pacific ocean, Microb. Ecol., 83, 916-928, https://doi.org/10.1007/s00248-021-01788-7, 2022.

Lindeque, P. K., Parry, H. E., Harmer, R. A., Somerfield, P. J., and Atkinson, A.: Next generation sequencing reveals the hidden diversity of zooplankton assemblages, PLoS One, 8, e81327, https://doi.org/10.1371/journal.pone.0081327, 2013.

Lopez-Garcia, P., Vereshchaka, A., and Moreira, D.: Eukaryotic diversity associated with carbonates and fluid-seawater interface in Lost City hydrothermal field, Environ. Microbiol., 9, 546-554, https://doi.org/10.1111/j.1462-2920.2006.01158.x, 2007.

Love, M. I., Huber, W., and Anders, S.: Moderated estimation of fold change and dispersion for RNA-seq data with DESeq2, Genome Biol., 15, 550, https://doi.org/10.1186/s13059-014-0550-8, 2014.

Luddington, I. A., Lovejoy, C., and Kaczmarska, I.: Species rich meta-communities of the diatom order Thalassiosirales in the Arctic and northern Atlantic Ocean, J. Plankton Res., 38, 781-797, https://doi.org/10.1093/plankt/fbw030 2016.

Marincovich, L., Barinov, K. B., and Oleinik, A. E.: The Astarte (Bivalvia Astartidae) that document the earliest opening of Bering Strait, J. Paleontol., 76, 239-245, https://doi.org/10.1666/0022-3360(2002)076<0239:Tabatd>2.0.Co;2, 2002.

Martrat, B., Grimalt, J. O., Villanueva, J., van Kreveld, S., and Sarnthein, M.: Climatic dependence of the organic matter contributions in the north eastern Norwegian Sea over the last 15,000 years, Org. Geochem., 34, 1057-1070, https://doi.org/10.1016/s0146-6380(03)00084-6, 2003.

Mylnikov, A. P., Weber, F., Jurgens, K., and Wylezich, C.: Massisteria marina has a sister: Massisteria voersi sp. nov., a rare species isolated from coastal waters of the Baltic Sea, Eur. J. Protistol., 51, 299-310, https://doi.org/10.1016/j.ejop.2015.05.002, 2015.

Newbold, L. K., Oliver, A. E., Booth, T., Tiwari, B., Desantis, T., Maguire, M., Andersen, G., van der Gast, C. J., and Whiteley, A. S.: The response of marine picoplankton to ocean acidification, Environ. Microbiol., 14, 2293-2307, https://doi.org/10.1111/j.1462-2920.2012.02762.x, 2012.

Nikolaev, S. I., Berney, C., Fahrni, J., Mylnikov, A. P., Aleshin, V. V., Petrov, N. B., and Pawlowski, J.: Gymnophrys cometa and Lecythium sp are core Cercozoa: Evolutionary implications, Acta Protozool., 42, 183-190, 2003.

Obiol, A., Del Campo, J., de Vargas, C., Mahe, F., and Massana, R.: How marine are Marine Stramenopiles (MAST)? A cross-system evaluation, FEMS Microbiol. Ecol., 100, https://doi.org/10.1093/femsec/fiae130, 2024.

Oksanen, J., Kindt, R., Legendre, P., O'Hara, B., Stevens, M., and Henry, H.: vegan: Community Ecology Package, 10, 719, 2007.

Paradis, E., Blomberg, S., Bolker, B., Brown, J., Claude, J., Cuong, H. S., Desper, R., and Didier, G.: ape: Analyses of Phylogenetics and Evolution, 2, 47, 2019.

Paulson, J. N., Stine, O. C., Bravo, H. C., and Pop, M.: Differential abundance analysis for microbial marker-gene surveys, Nat. Methods, 10, 1200-1202, https://doi.org/10.1038/nmeth.2658, 2013.

https://doi.org/10.5194/egusphere-2025-3780
Preprint. Discussion started: 18 August 2025

Pawlowska, J., Wollenburg, J. E., Zajaczkowski, M., and Pawlowski, J.: Planktonic foraminifera genomic variations reflect paleoceanographic changes in the Arctic: evidence from sedimentary ancient DNA, Sci. Rep., 10, 15102, https://doi.org/10.1038/s41598-020-72146-9, 2020.

Petersen, G. H.: Studies on some Arctic and Baltic Astarte species (Bivalvia, Mollusca), Museum Tusculanum Press2001.

Petz, W., Song, W., and Wilbert, N.: Taxonomy and ecology of the ciliate fauna (Protozoa, Ciliophora) in the endopagial and pelagial of the Weddell Sea, Antarctica, Land Oberösterreich, OÖ Landesmuseum1995.

Polyakov, I. V., Rippeth, T. P., Fer, I., Alkire, M. B., Baumann, T. M., Carmack, E. C., Ingvaldsen, R. B., Ivanov, V. V., Janout, M., Lind, S., Padman, L., Pnyushkov, A. V., and Rember, R.: Weakening of cold Halocline layer exposes sea ice to Oceanic heat in the eastern Arctic Ocean, J. Clim., 33, 8107-8123, https://doi.org/10.1175/jcli-d-19-0976.1, 2020.

Polyakov, I. V., Pnyushkov, A. V., Alkire, M. B., Ashik, I. M., Baumann, T. M., Carmack, E. C., Goszczko, I., Guthrie, J., Ivanov, V. V., Kanzow, T., Krishfield, R., Kwok, R., Sundfjord, A., Morison, J., Rember, R., and Yulin, A.: Greater role for Atlantic inflows on sea-ice loss in the Eurasian Basin of the Arctic Ocean, Science, 356, 285-291, https://doi.org/10.1126/science.aai8204, 2017.

Ribeiro, C. G., Lopes dos Santos, A., Trefault, N., Marie, D., Lovejoy, C., and Vaulot, D.: Arctic phytoplankton microdiversity across the marginal ice zone: Subspecies vulnerability to sea-ice loss, Elem Sci Anth, 12, https://doi.org/10.1525/elementa.2023.00109, 2024.

Rintala, J.-M., Hällfors, H., Hällfors, S., Hällfors, G., Majaneva, M., and Blomster, J.: Heterocapsa Arctica Subsp. Frigida Subsp. Nov. (Peridiniales, Dinophyceae)-Description of a New Dinoflagellate and Its Occurrence in the Baltic Sea1, J. Phycol., 46, 751-762, https://doi.org/10.1111/j.1529-8817.2010.00868.x, 2010.

Risebrobakken, B., Moros, M., Ivanova, E. V., Chistyakova, N., and Rosenberg, R.: Climate and oceanographic variability in the SW Barents Sea during the Holocene, The Holocene, 20, 609-621, https://doi.org/10.1177/0959683609356586, 2010.

Roberts, D. W.: Statistical analysis of multidimensional fuzzy set ordinations, Ecology, 89, 1246-1260, https://doi.org/10.1890/07-0136.1, 2008.

Rueckert, S., Wakeman, K. C., Jenke-Kodama, H., and Leander, B. S.: Molecular systematics of marine gregarine apicomplexans from Pacific tunicates, with descriptions of five novel species of Lankesteria, Int. J. Syst. Evol. Microbiol., 65, 2598-2614, https://doi.org/10.1099/ijs.0.000300, 2015.

Schweikert, M. and Schnepf, E.: Light and electron microscopical observations on Pirsonia punctigerae spec, nov., a nanoflagellate feeding on the marine centric diatom Thalassiosira punctigera, Eur. J. Protistol., 33, 168-177, https://doi.org/10.1016/S0932-4739(97)80033-8, 1997.

Skogseth, R., Olivier, L. L. A., Nilsen, F., Falck, E., Fraser, N., Tverberg, V., Ledang, A. B., Vader, A., Jonassen, M. O., Søreide, J., Cottier, F., Berge, J., Ivanov, B. V., and Falk-Petersen, S.: Variability and decadal trends in the Isfjorden (Svalbard) ocean climate and circulation – An indicator for climate change in the European Arctic, Prog. Oceanogr., 187, https://doi.org/10.1016/j.pocean.2020.102394, 2020.

Stoecker, D. K. and Lavrentyev, P. J.: Mixotrophic Plankton in the Polar Seas: A Pan-Arctic Review, Front. Mar. Sci., 5, https://doi.org/10.3389/fmars.2018.00292, 2018.

Sundfjord, A., Albretsen, J., Kasajima, Y., Skogseth, R., Kohler, J., Nuth, C., Skarðhamar, J., Cottier, F., Nilsen, F., Asplin, L., Gerland, S., and Torsvik, T.: Effects of glacier runoff and wind on surface layer dynamics and Atlantic Water exchange in Kongsfjorden, Svalbard; a model study, Estuar. Coast. Shelf Sci., 187, 260-272, https://doi.org/10.1016/j.ecss.2017.01.015, 2017.

Team, R. C.: A language and environment for statistical computing [code], 2013.

https://doi.org/10.5194/egusphere-2025-3780
Preprint. Discussion started: 18 August 2025

Telesiński, M. M., Kucharska, M., Łącka, M., and Zajączkowski, M.: A late response of the sea-ice cover to Neoglacial cooling in the western Barents Sea, The Holocene, 34, 1088-1096, https://doi.org/10.1177/09596836241247305, 2024.

Telesiński, M. M., Przytarska, J. E., Sternal, B., Forwick, M., Szczuciński, W., Łącka, M., and Zajączkowski, M.: Palaeoceanographic evolution of the SW Svalbard shelf over the last 14 000 years, Boreas, 47, 410-422, 10.1111/bor.12282, 2017.

Thomsen, H. A. and Ostergaard, J. B.: Acanthoecid choanoflagellates from the Atlantic Arctic Region - a baseline study, Heliyon, 3, e00345, https://doi.org/10.1016/j.heliyon.2017.e00345, 2017.

Tillmann, U., Wietkamp, S., Gottschling, M., and Hoppenrath, M.: Prorocentrum pervagatum sp. nov. (Prorocentrales, Dinophyceae): A new, small, planktonic species with a global distribution, Phycol. Res., 71, 56-71, https://doi.org/10.1111/pre.12502, 2022.

Wassmann, P., Duarte, C. M., AgustÍ, S., and Sejr, M. K.: Footprints of climate change in the Arctic marine ecosystem, Glob. Chang. Biol., 17, 1235-1249, https://doi.org/10.1111/j.1365-2486.2010.02311.x, 2010.

Wei, T. and Simko, V.: R Package "Corrplot": Visualization of a Correlation Matrix (Version 0.95) [code], 2024.

Wickham, H.: ggplot2: Elegant Graphics for Data Analysis, Springer-Verlag New York2016.

Wickham, H.: stringr: Simple, Consistent Wrappers for Common String Operations [code], 2019.

Wilbert, N. and Song, W.: A further study on littoral ciliates (Protozoa, Ciliophora) near King George Island, Antarctica, with description of a new genus and seven new species, J. Nat. Hist., 42, 979-1012, https://doi.org/10.1080/00222930701877540, 2008.

Wollenburg, J. E., Knies, J., and Mackensen, A.: High-resolution paleoproductivity fluctuations during the past 24 kyr as indicated by benthic foraminifera in the marginal Arctic Ocean, Palaeogeogr., Palaeoclimatol., Palaeoecol., 204, 209-238, https://doi.org/10.1016/s0031-0182(03)00726-0, 2004.

Wu, X., Liu, Y., Weng, Y., Li, L., and Lin, S.: Isolation, identification and toxicity of three strains of Heterocapsa (Dinophyceae) in a harmful event in Fujian, China, Harmful Algae, 120, 102355, https://doi.org/10.1016/j.hal.2022.102355, 2022.

Xu, D., Song, W., and Hu, X.: Morphology of Cyclotrichium taniguchii sp. nov. and C. cyclokaryon with establishment of a new genus, Dicyclotrichium gen. nov. (Ciliophora: Haptorida), J. Mar. Biol. Assoc. U.K., 85, 787-794, https://doi.org/10.1017/s0025315405011719, 2005.

Zajaczkowski, M.: Sediment supply and fluxes in glacial and outwash fjords, Kongsfjorden and Adventfjorden, Svalbard, Polish Polar Research, 29, 59-72, 2008.

Zimmermann, H. H., Stoof-Leichsenring, K. R., Kruse, S., Nürnberg, D., Tiedemann, R., and Herzschuh, U.: Sedimentary Ancient DNA From the Subarctic North Pacific: How Sea Ice, Salinity, and Insolation Dynamics Have Shaped Diatom Composition and Richness Over the Past 20,000 Years, Paleoceanography and Paleoclimatology, 36, https://doi.org/10.1029/2020pa004091, 2021.

Zimmermann, H. H., Stoof-Leichsenring, K. R., Dinkel, V., Harms, L., Schulte, L., Hutt, M. T., Nurnberg, D., Tiedemann, R., and Herzschuh, U.: Marine ecosystem shifts with deglacial sea-ice loss inferred from ancient DNA shotgun sequencing, Nat Commun, 14, 1650, https://doi.org/10.1038/s41467-023-36845-x, 2023.